Strain index: A new visualizing parameter for US elastography - art. no. 69200W

Article *in* Proceedings of SPIE - The International Society for Optical Engineering · September 2008

DOI: 10.1117/12.769191

5 authors, including:

Rodrigo De Luis-García
Universidad de Valladolid
82 PUBLICATIONS **790** CITATIONS

SEE PROFILE

Carlos Alberola-López
Universidad de Valladolid
240 PUBLICATIONS **2,843** CITATIONS

SEE PROFILE

Juan Ruiz-Alzola
Universidad de Las Palmas de Gran Canaria
94 PUBLICATIONS **1,229** CITATIONS

SEE PROFILE

Strain Index: a New Visualizing Parameter for US Elastography

Dario Sosa-Cabrera[a], R. de Luis-García[b],A. Tristán-Vega[b],
Carlos Alberola-López[b] and Juan Ruiz-Alzola[c,a]

[a]Center for Technology in Medicine, Dept. Señales y Comunicaciones,
University of Las Palmas de Gran Canaria, SPAIN
Lab. 203, Pabellón B, Edificio de Telecomunicaciones
Campus de Tafira s/n. 35017 Las Palmas
email: dario@ctm.ulpgc.es

[b]Laboratory of Image Processing, Dept. Teoría de la Señal
University of Valladolid, SPAIN
Edificio de las Nuevas Tecnologías
Campus Miguel Delibes s/n. 47011 Valladolid
email: {rodlui, caralb}@lpi.tel.uva.es

[c]Canarian Agency for R+D and Information Technologies, SPAIN
C/ Cebrián, n 3. 35071 Las Palmas de Gran Canaria
email: jruiz@itccanarias.org

ABSTRACT

Elastography, an ultrasound modality based on the relation between tissue strain and its mechanical properties, has a strong potential in the diagnosis and prognosis of tumors. For instance, tissue affected by breast and prostate cancer undergoes a change in its elastic properties. These changes can be measured using ultrasound signals.

The standard way to visualize the elastic properties of tissues in elastography is the representation of the axial strain. Other approaches investigate the information contained in shear strain elastograms, vorticity or the representation of the full strain tensor. In this paper, we propose to represent the elastic behaviour of tissues through the visualization of the *Strain Index*, related with the trace of the strain tensor. Based on the mathematical interpretation of the strain tensor, this novel parameter is equivalent to the sum of the eigenvalues of the strain tensor, and constitutes a measure of the total amount of strain of the soft tissue.

In order to show the potential of this visualization approach, a tissue-mimicking phantom was modeled as a 10x10x5 cm region containing a centered 10mm cylindrical inclusion three times stiffer than the surrounding material, and its elastic behavior was simulated using finite elements software. Synthetic pre- and post-compression (1.25%) B-mode images were computer-generated with ultrasound simulator. Results show that the visualization of the tensor trace significantly improves the representation and detection of inclusions, and can help add insight in the detection of different types of tumors.

Keywords: Elastography, Elasticity Imaging, Elastogram, Strain, Trace, Medical Imaging, Ultrasound, Optical Flow.

1. INTRODUCTION

Changes in tissue stiffness correlate with pathological phenomena that can aid the diagnosis of several diseases such as breast and prostate cancer [1,2] or cardiovascular dysfunctions.[3,4] For example, scirrhous carcinoma appears frequently as a hard nodule in the breast tissue and a liver tissue with cirrhosis is stiffer than the normal tissue. Many different approaches try to estimate and image the elastic properties of tissues, but this is not

Medical Imaging 2008: Ultrasonic Imaging and Signal Processing, edited by Stephen A. McAleavey, Jan D'hooge, Proc. of SPIE Vol. 6920, 69200W, (2008) · 1605-7422/08/$18 · doi: 10.1117/12.769191

possible with conventional ultrasound, MRI, CT or nuclear imaging. There are mechanical ways to estimate the biomechanical properties of the tissue such as indentation, which is mostly used for thin layers of tissue ex-vivo.[5,6]

Palpation is an effective method used for decades for lesion detection and evaluation; with this motivation researchers had tried to reproduce this method making it subject independant. Elastography, is an imaging technique whereby, the tissue response to some stimulus affecting its elastic state, is estimated. It is well established in the literature. Ophir et al.,[7] proposed in 1991 the use of ultrasound together with a mechanical quasi-static compression in order to estimate the elasticity of different tissues.

The standard way of visualizing the elastic properties in elastography is the axial strain. The lateral strain,[7] Poisson's ratio,[8] shear strain,[9] or vorticity[10] elastograms are also visualized. The *inverse problem* approach deals with Young's modulus visualization, the shear modulus[11] or other related parameters. Some recent investigations visualize the whole strain tensor as ellipsoids[12] Other techniques such as sonoelastography,[13] visualizes the propagating acoustic waves. All of these visualizations have in common the intentionality to differentiate different stiffness regions, or different elastic behaviors of the tissues.

Although elastography has been shown to be capable of detecting breast tumors in vivo,[1] biopsies are still needed to assess their malignancy. Malignant tumors are known to form ramified boundaries that become firmly bound to the surrounding tissue, as opposed to the benign ones, which have smooth borders and are loosely attached to its surrounding.[1] and[9] have made efforts trying to reduce the use of biopsies, with US elastography.

The purpose of this work is to add another way for visualizing the elastic properties of the tissues in order to give more information to the clinicians. The *Strain Index* proposed in this work is derived from the trace of the strain tensor, thus providing a more global insight as it takes information from both the axial and the lateral strain, and is more precise detecting the boundaries of hard masses as the experiments have shown.

This work is organized as follows. In Section 2, we present the mathematical basis from where we obtain the new parameters that we will use for visualization and the experimental set-up. We expose in Section 3 the motivation and preliminary investigations that made us deepen in this research and their results, discussing the visualization methods. Finally, in Section 4 the conclusions are related and the future work is also outlined.

2. METHODS

2.1 Mathematics

Let $\mathbf{u} = (u_x, u_y)$ be a 2-D displacement vector field. It is well known from mechanical engineering that the *displacement gradient matrix*, also called *Jacobian matrix* or *unit relative displacement matrix* can be decomposed into the *strain tensor*, which is the symmetric part, and the vorticity tensor, which is the antisymmetric part:[14]

$$\mathbf{J} = \nabla\mathbf{u} = \begin{pmatrix} \frac{\partial u_x}{\partial x} & \frac{\partial u_x}{\partial y} \\ \frac{\partial u_y}{\partial x} & \frac{\partial u_y}{\partial y} \end{pmatrix} = \mathbf{E} + \mathbf{\Omega} \tag{1}$$

The strain tensor $\mathbf{E}$, with the elongational strains on the diagonal and the shearing strains off the diagonal, measures the changes of shape locally (stretching or shortening), while the vorticity matrix $\mathbf{\Omega}$ contains information about rotations.
In this work, we propose a novel parameter to visualize the elastic properties of the tissue. To that order, let us perform the eigenvalue decomposition of the strain tensor $\mathbf{E}$:

$$\mathbf{E} = \mathbf{V}\mathbf{D}\mathbf{V}^{-1} = \begin{pmatrix} v_{11} & v_{21} \\ v_{12} & v_{22} \end{pmatrix} \begin{pmatrix} d_1 & 0 \\ 0 & d_2 \end{pmatrix} \begin{pmatrix} v_{11} & v_{21} \\ v_{12} & v_{22} \end{pmatrix}^{-1} \tag{2}$$

where v_{ij} is the j-th component of the eigenvector associated with the eigenvalue d_i. Following the analysis performed in the field of DT-MRI (*Diffusion Tensor Magnetic Resonance Imaging*), the sum of the eigenvalues of the diffusion tensor (which is a symmetric positive definite –SPD– tensor) gives information about the total amount of diffusion that takes place in the tissue. Similarly, the sum of the eigenvalues of the strain tensor gives information about the total amount of strain in the tissue. The strain tensor, however, is not always

a SPD matrix, and negative eigenvalues can appear depending on the choice of the coordinate system. This problem can be easily overcome by taking the absolute value of the eigenvalues considered. Thus, we propose the representation of the elastic information of tissues in elastography through *Strain Index*, SI, which is defined as follows:

$$SI = \sum \mid d_i \mid \tag{3}$$

where d_i are the eigenvalues. For the general 3D case, the SI is the sum of the absolute values of the three eigenvalues of the strain tensor matrix.

$$SI = |d_1| + |d_2| \tag{4}$$

In our 2D case, we have represented the sum of the absolute value of the two eigenvalues d_1 and d_2.

2.2 Settings

We have developed an experimental setting that has proved to be very useful in order to obtain preliminary results, prior to clinical experimentation. This setting allows us to easily experiment under different conditions and mechanical characteristics that we expect to correlate with real clinical data. Two experimental phantoms were devised to progressively take into account both the elastic response of the tissue and the dynamic range of conventional ultrasound images: simulated data generated with finite element analysis software (phantom A), and computer-simulated ultrasound images (phantom B).

Phantom A. A virtual phantom was modelled as a $10x10x5\ cm^3$ region containing a centered cylindrical inclusion, 10 mm in diameter and five times stiffer than the uniformly elastic surrounding material (21 KPa).[5] For both inclusion and surrounding tissue, the Poisson's ratio used was v = 0.495.[5] Both lateral sides of the phantom are free to move. Its elastic deformation, caused by applying a 2,5% uniform uniaxial compression, was simulated using finite elements software. The visualization of the strain of this phantom is considered as ground truth.

Phantom B. Complementing the former, another virtual phantom with a uniform distribution of approximately 150.000 ultrasound scatterers with random amplitudes was created. The mechanical deformation produced in Phantom A with the FE simulation, was reproduced by displacing each scatterer. Synthetic pre- and post-compression B-mode images were generated using FIELD II ultrasound simulator.

2.3 Analysis

Different approaches have been developed to estimate and image the elastic properties of tissue. All of them estimate a displacement vector field due to an applied deformation load. In ultrasound elastography, the estimation of the displacement and strain fields is mostly based on measurements performed on the RF signals (time-domain cross-correlation, among others). Pellot-Barakat et al.[15] have proposed a multi-scale optical flow method where the estimation of regularized displacement fields is obtained from two consecutive B-mode images. Following this idea, we have used a multi-scale variational method to estimate the displacement field, but our method uses a regularization term that allows preservation of discontinuities in the flow. We are able to obtain a better estimation on the boundaries of the inclusions in the tissue with our method. Further information on this issue can be found in our previous work.[16,17]

From the estimated displacement field we create its correspondent vector field. To obtain the derivatives we have used a least-squares strain estimator using 12 mm window size (typically used for real-time elastography) which gives the best performance as presented in our work,[17] obtaining the Jacobian matrix. Afterwards, we decompose it in the strain and the vorticity tensor fields.

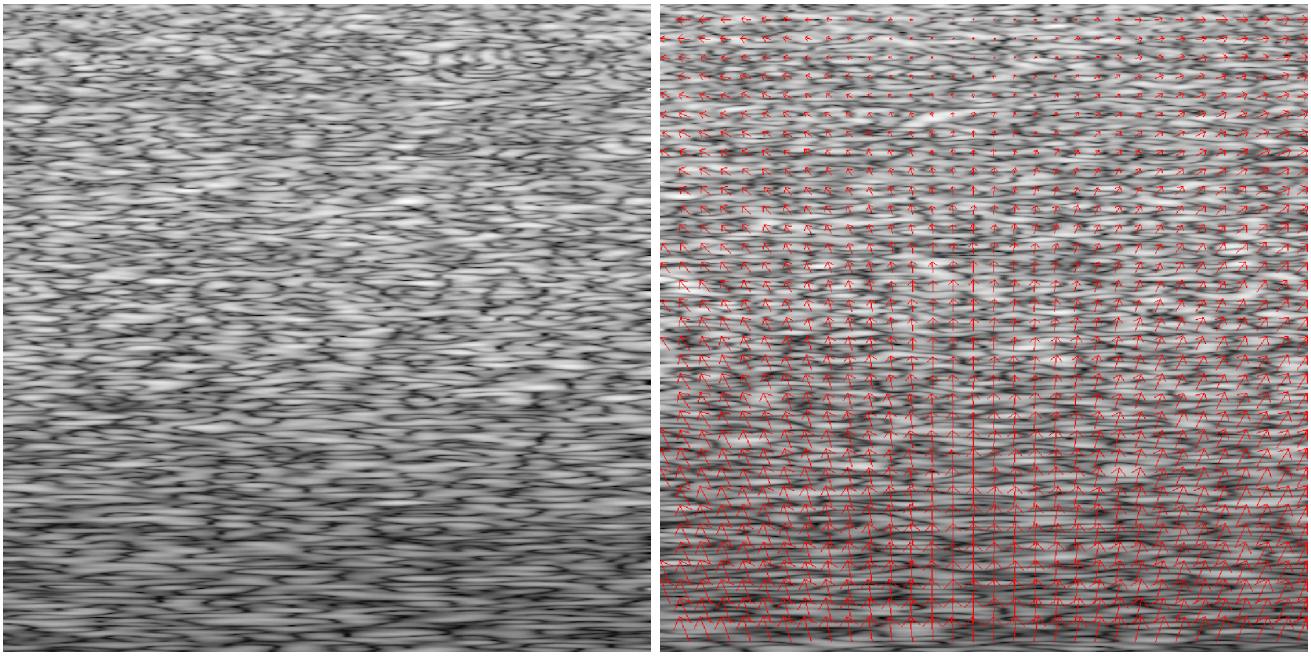

Figure 1. *Left:* Precompression B-mode image from FIELD II. *Right:* Vector field of the displacement estimation overimpossed to the B-mode ultrasound simulated image.

3. RESULTS

In this work, we have employed a multiscale variational optical flow method to estimate the displacement field described in.[16] The isoechoic input precompression image, is presented in Figure 1, together with the displacement field estimation represented with the vectors overlaid to the B-mode image. It can be observed that the inclusion cannot be appreciated in the B-mode image. The strain image of phantom A, considered the ground truth is shown in figure 2.

The resulting elastograms are presented in Figures 3 and 4. Both elastograms present the inclusion clearly visible. If we compare the ground truth strain image (Figure 1) with both elastograms (Figures 3 and 4), it can be appreciated that the shape of the inclusion is more accurate with the SI representation. While the inclusion has been designed as perfectly circular, the axial elastograms gives a more squared result, however the SI representation yields a circular inclusion, still not perfectly circular but with a closer shape, compared to the ground truth strain image. At the same time, the area inside the inclusion of the latter elastogram is more homogeneous as it avoids the softer patterns that appear in the former. This makes us think that the CNRe (elastographic contrast to noise ratio) will be higher for the SI visualizations.

The boundaries are also clearer on the latter. On the strain elastogram (Figure 3), an undesired vertical pattern is observed which does not appear with the novel SI representation. This difference in a synthetic experiment might be crucial in an in-vivo case. This visualization of the SI can help the physicians with complementary information to detect different lesions. Furthermore, the expected improvement in the elastogram quality will allow the intoduction of segmentation methods on the elastography images in order to detect the borders of the inclusions. This task is still very difficult with the quality of the elastograms obtained before. The SI, as seen in section 2.1, is related to the properties of the strain tensor. New parameters derived from the algebraic interpretation of the strain, and the full second order tensor as it is, may be investigated following the approach presented in this work.

4. CONCLUSION AND ON-GOING RESEARCH

A deeper comparison with other visualization parameters is needed as well as clinical validation with in-vivo experiments. An intermediate step will be to test the SI visualization with comercial phantoms scanned with

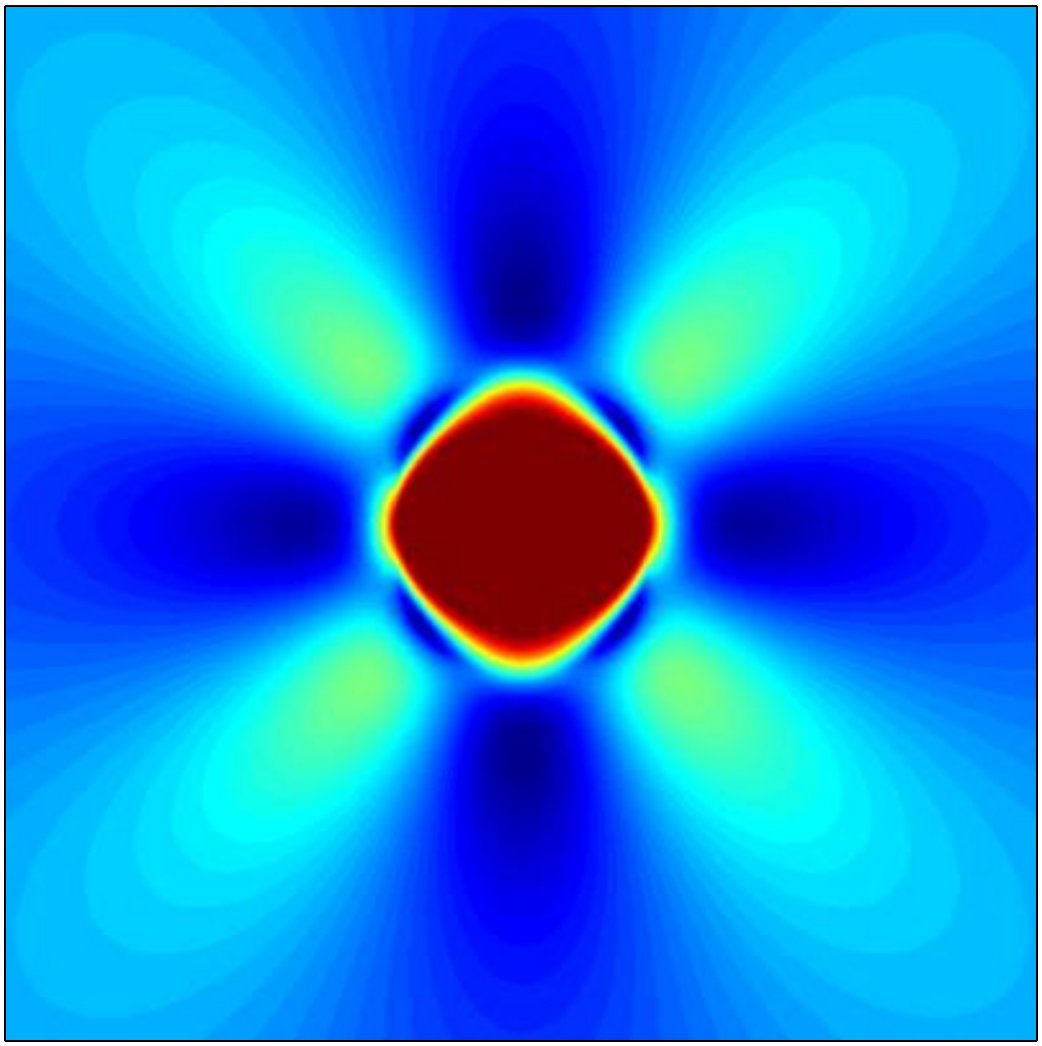

Figure 2. Phantom A strain image considered the ground truth.

conventional equipment. An study of the boundary conditions affecting this visualization and compared to the axial strain elastograms is also proposed[18] to add insight on the properties of the strain index. Once the clinical validation is achieved, the final goal is to provide physicians with different visualization methods incorporated in a standard scanner in order to allow them to employ the visualization technique that best fits for each situation or to obtain complementary information from different visualization methods. During the early development of elasticity imaging the standard parameters used to visdualize the elastic characteristics of a tissue have been parameters of the strain or elasticity tensor. With the development of hardware capacity in informatics, new possibilities had been studied. The experiments presented show that the Strain Index visualizes a hard inclusion preserving its shape in a better manner as compared to the axial strain.

Acknowledgments. Funding was provided by the Spanish Ministry of Science and Technology (TEC-2004-06647-C03-02) and the European NoE SIMILAR FP6-507609.

REFERENCES

1. B. Garra, I. Céspedes, J. Ophir, S. Spratt, R. A. Zuurbier, C. M. Magnant, and M. F. Pennanen, "Elastography of breast lesions: initial clinical results," *Radiology* **202**, pp. 79–86, 1997.

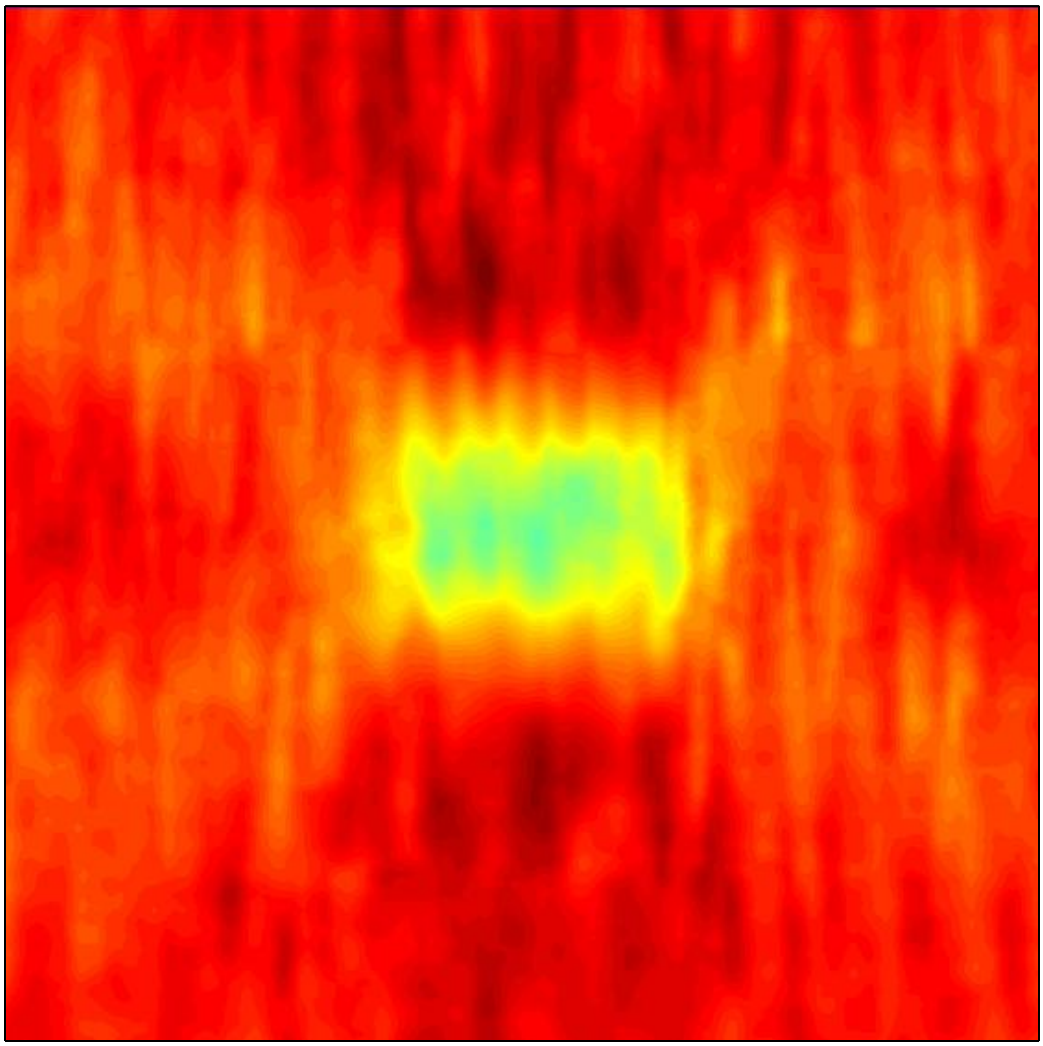

Figure 3. Axial Strain elastogram.

2. K. M. Hiltawsky, M. Kruger, C. Starke, L. Heuser, H. Ermert, and A. Jensen, "Freehand ultrasound elastography of breast lesions: Clinical results," *Ultrasound Med. Biol.* **27**, pp. 1461–1469, 2001.
3. M. Shling, M. Arigovindan, C. Jansen, P. Hunziker, and M. Unser, "Myocardial motion analysis from b-mode echocardiograms," *IEEE Transactions on Image Processing* **14**, April 2005.
4. R. Maurice, M. Daronat, J. Ohayon, E. Stoyanova1, F. Foster, and G. Cloutier, "Non-invasive high-frequency vascular ultrasound elastography," *Phys. Med. Biol.* **50**, pp. 1611–1628, 2005.
5. T. Krouskop, T. Wheeler, F. Kallel, B. Garra, and T. Hall, "Elastic moduli of breast and prostate tissue under compression," *Ultrasonic Imaging* **20**, pp. 260–274, 1998.
6. S. Srinivasan, T. Krouskop, and J. Ophir, "Comparing elastographic strain images with modulus images obtained using nano-indentation: Preliminary results using phantoms and tissue samples," *Ultrasound in Medicine and Biology* **30**(3), pp. 329–343, 2004.
7. J. Ophir, I. Céspedes, B. Garra, H. Ponnekanti, Y. Huang, and N. Maklad, "Elastography: a quantitative method for imaging the elasticity of biological tissues," *Ultrasound Imaging* **13**, pp. 111–134, 1991.
8. R. Righetti, J. Ophir, S. Srinivasan, and T. Krouskop, "The feasibility of using elastography for imaging the poisson's ratio in porous media," *Ultrasound in Medicine and Biology* **30**(2), pp. 215–228, 2004.

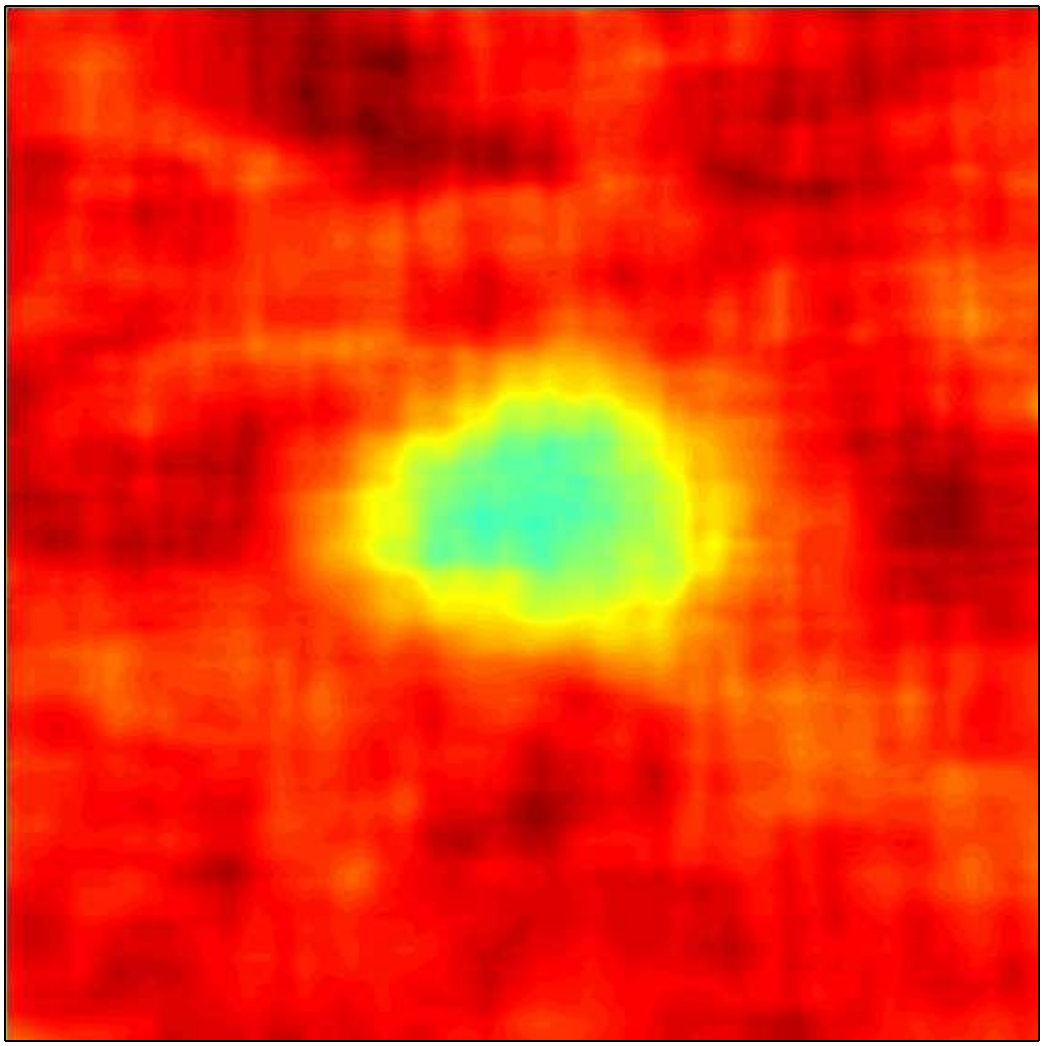

Figure 4. SI elastogram.

9. E. Konofagou, T. Harrigan, and J. Ophir, "Shear strain estimation and lesion mobility assessment in elastography," *Ultrasonics* **38**, pp. 400–404, 2000.
10. D. Sosa-Cabrera, M. Rodriguez-Florido, E. Suarez-Santana, and J. Ruiz-Alzola, "Vorticity visualization: Phantom study for a new discriminant parameter in elastography," in *Proceedings of SPIE in Medical Imaging*, **6513**(20), 2007.
11. M. Doyley, S. Srinivasan, S. Pendergrass, Z. Wu, and J. Ophir, "Comparative evaluation of strain-based and model-based modulus elastography," *Ultrasound in Medicine and Biology* **31**(6), pp. 787–802, 2005.
12. D. Sosa-Cabrera, J. Gonzalez-Fernandez, L. Gomez-Deniz, and J. Ruiz-Alzola, "Strain tensor elastography based on optical flow estimation of displacements fields," in *Proceedings of the Sixth International Conference on the Ultrasonic Measurement and Imaging of Tissue Elasticity*, p. 148, 2007.
13. R. Lerner and K. Parker, "Sonoelasticity imaging," in *Proceedings of the 16th International Acoustical Imaging Symposium (Plenum)*, **16**, pp. 317–327, (The Netherlands. Luxembourg), 1998.
14. L. Malvern, *Introduction to the Mechanics of a Continuous Medium*, Ed. Prentice Hall, 1969.
15. C. Pellot-Barakat, F. Frouin, M. Insana, and A. Herment, "Ultrasound elastography based on multiscale estimations of regularized displacement fields," *IEEE Transactions on Medical Imaging* **23**, pp. 153–163, February 2004.

16. D. Sosa-Cabrera, J. Gonzalez-Fernandez, C. C. no Moraga, L. Gomez-Deniz, L. Alvarez-Leon, and J. Ruiz-Alzola, "A multiscale variational optical flow method to estimate discontinuous motion fields for ultrasound elastography," in *Proceedings of Fifth the International Conference on the Ultrasonic Measurement and Imaging of Tissue Elasticity*, p. 31, 2006.
17. D. Sosa-Cabrera, J. Gonzalez-Fernandez, L. Gomez-Deniz, and J. Ruiz-Alzola, "Characterization of a multiscale variational optical flow method for elastography," in *Proceedings of the IEEE Ultrasonics International Symposium*, 2007.
18. D. Sosa-Cabrera, J. Ophir, T. Krouskop, A. Thitai-Kumar, and J. Ruiz-Alzola, "Study of the effect of boundary conditions and inclusion's position on the contrast transfer efficiency in elastography," in *IV International Conference on the Ultrasonic Measurement and Imaging of Tissue Elasticity*, p. 94, October 2005.